sustainability

MDPI

Article

Efficient Degradation of Carbendazim by Ferrate(VI) Oxidation under Near-Neutral Conditions

Yu Li and Hefa Cheng *

MOE Laboratory for Earth Surface Processes, College of Urban and Environmental Sciences, Peking University, Beijing 100871, China

* Correspondence: hefac@umich.edu; Tel.: +86-10-6276-1070

Abstract: Carbendazim (CBZ), a widely used fungicide in agriculture, is frequently detected in aquatic environment and causes significant concerns because of its endocrine-disrupting activity. This study investigated the degradation kinetics of CBZ in ferrate (Fe(VI)) oxidation, the influence of water matrices, and the transformation pathways of CBZ. The second-order rate constant for the reaction between CBZ and Fe(VI) decreased from 88.0 $M^{-1}{\cdot}s^{-1}$ to 1.6 $M^{-1}{\cdot}s^{-1}$ as the solution pH increased from 6.2 to 10.0. The optimum reaction conditions were obtained through response surface methodology, which were pH = 7.8 and [Fe(VI)]/[CBZ] = 14.2 (in molarity), and 96.9% of CBZ could be removed under such conditions. Cu^{2+} and Fe^{3+} accelerated the degradation of CBZ by Fe(VI) oxidation; common cations and anions found in natural water had no significant effect, while the presence of humic acid also accelerated the degradation of CBZ. Based on the degradation products identified, degradation of CBZ in Fe(VI) oxidation proceeded via three pathways: namely, hydroxylation, removal of the methoxyl group, and cleavage of the C–N/C=N bond. The initial reaction site of CBZ oxidation by Fe(VI) was also supported by the atomic partial charge distribution on the CBZ molecule obtained from density functional theory (DFT) calculations. CBZ in natural water matrices was efficiently removed by Fe(VI) oxidation under near-neutral conditions, indicating that Fe(VI) oxidation could be a promising treatment option for benzimidazole fungicides.

Keywords: carbendazim; ferrate; oxidation kinetics; degradation pathways; water treatment; water matrices

Citation: Li, Y.; Cheng, H. Efficient Degradation of Carbendazim by Ferrate(VI) Oxidation under Near-Neutral Conditions. *Sustainability* **2022**, *14*, 13678. https://doi.org/10.3390/su142013678

Academic Editor: Elena Cristina Rada and Ioannis Katsoyiannis

Received: 22 August 2022
Accepted: 20 October 2022
Published: 21 October 2022

1. Introduction

Carbendazim (methyl-1-H-benzimidazole-2-ylcarbamate, CBZ) is a typical benzimidazole fungicide that is widely used to prevent the effects of harmful pathogens on crops, fruits, and vegetables [1,2]. It is also known as the main degradation product of two other benzimidazole fungicides, benomyl and thiophanate-methyl [3,4]. CBZ is stable and persistent in the environment [3,5,6]; thus, it is widely detected in aquatic environment [1,7–12]. For example, the concentration of CBZ is up to 607 $ng{\cdot}L^{-1}$ in the Huangpu River, China, and up to 0.58 ng L^{-1} in the tap water of northern Vietnam [13]. Very high concentrations of CBZ, ranging from 0.11 mg L^{-1} to 0.18 mg L^{-1}, were detected in paddy field water soon after its application (1 h) [14]. It has been reported that CBZ can act as an endocrine disruptor [1,3] and has liver toxicity [15,16]. Given its wide occurrence and toxic effects, there is a significant need to develop efficient treatment technologies for removing CBZ from water.

Common treatment processes for the removal of organic pollutants from water mainly include photolysis, biodegradation, adsorption, and chemical oxidation [3,17,18]. Both photolysis and biodegradation have rather low efficiency in the removal of CBZ [19]. While adsorption only transfers CBZ from the liquid phase to the solid phase, it does not destruct the pollutants. Advanced oxidation processes (AOPs) have been proven to be effective in treating refractory organic pollutants due to the production of highly active hydroxyl radicals (•OH) [18,20]. da Costa et al. applied the solar photo-Fenton process to remove

CBZ from water and found that over 96% removal could be achieved within 15 min [21]. However, Fenton-type processes usually require acidic media, which are not desirable in water treatment. Mazellier et al. reported that rapid degradation of CBZ can occur in the UV/H_2O_2 process [22]. Photocatalytic processes were also employed for the treatment of CBZ from water, which achieved satisfactory performance [23]. However, the high cost of UV irradiation limits the application of these processes, and the photocatalysts are also not commercially available. Recently, Xu et al. compared the degradation of CBZ by $KMnO_4$ activated with benzoquinone and bisulfite and found that both processes could achieve good results. However, $KMnO_4$ oxidation brings the undesirable product Mn^{2+}, which needs to be controlled with the further addition of chemicals [24].

Ferrate (Fe(VI)) is a strong oxidant that has excellent performance in water and wastewater treatment, including oxidation, flocculation, sterilization, and disinfection [25–32]. It is capable of oxidizing organic pollutants that have unsaturated functional groups, especially nitrogen- and sulfur-containing compounds [33–35]. Compared to other water and wastewater treatment processes, Fe(VI) oxidation has the advantages of simple operation, fast oxidation rate, low cost, and good performance under near-neutral conditions. Xie et al. comprehensively compared the performance and cost of Fe(VI) oxidation and the Fenton process using *p*-arsanilic acid as the model pollutant and found that Fe(VI) oxidation has the advantages of shorter treatment time and lower capital cost [32]. Unlike other AOPs that are based on active free radicals, Fe(VI) oxidation of organic pollutants is hardly inhibited by the co-existing ions and dissolved organic matter (DOM) [36], and it performs well in natural water under near-neutral conditions [37]. Nonetheless, while studies have demonstrated promising treatment results for the oxidation of organic pollutants in drinking water by Fe(VI) [38,39], the relatively high cost of Fe(VI) currently limits its practical application, and further research is required to reduce the treatment's operating cost.

This study aimed to investigate the kinetics and mechanism of CBZ degradation in Fe(VI) oxidation and the influence of water matrices. The effects of oxidant dose and pH were studied, and the optimum oxidation conditions were established through response surface optimization experiments. The order and rate constant of the reaction between Fe(VI) and CBZ were determined. The degradation of CBZ by Fe(VI) oxidation was further examined in the presence of common ions and humic acid (HA), as well as in natural water matrices. Finally, the degradation pathways and mechanism of CBZ by Fe(VI) oxidation were proposed based on the experimental results and theoretical calculations. The findings of this study can guide the practical treatment of benzimidazole fungicides in water and wastewater by Fe(VI) oxidation.

2. Materials and Methods

2.1. Chemicals and Reagents

CBZ (98%), 2,2-azino-bis(3-ethylbenzothiazoline)-6-sulfonate (ABTS, >98%), and borate (GR) were obtained from Macklin Biochemical (Shanghai, China). NaCl, KCl, NaBr, $NaNO_3$, $NaHCO_3$, NaH_2PO_4, Na_2HPO_4, and Na_2CO_3 were purchased from Sinopharm Chemical Reagent (Shanghai, China). $CaCl_2$, $MgCl_2$, $CuCl_2$, and $FeCl_3$ were provided by Kemiou Chemical Reagent (Tianjin, China). HA was supplied by Sigma-Aldrich (St. Louis, MO, USA). Unless noted otherwise, ultrapure water (18.2 MΩ cm) produced from a Milli-Q Reference system (Millipore, Bedford, MA, USA) was used in the preparation of all solutions.

Fe(VI) was prepared according to the wet chemical method reported in the literature [40], and the purity was higher than 90%. As a dry solid, the K_2FeO_4 prepared was stable, but it would decompose in contact with water. The purity of K_2FeO_4 synthesized was determined from absorbance measurement (at 510 nm) of the Fe(VI) solution prepared from dissolution of the powder in a buffer solution of 1 mM $Na_2B_4O_7$/5 mM Na_2HPO_4 (pH 9.2) and comparison with the known molar absorptivity of Fe(VI) at pH above 9.0 ($\varepsilon_{510\ nm}$ = 1150 M^{-1} cm^{-1} [41,42]). The stock solutions of Fe(VI) were prepared by dissolving solid Fe(VI) in phosphate or borate buffer, depending on the pH of the solutions to

be studied. The stock solution of CBZ was prepared by dissolving solid CBZ in ultrapure water with the addition of HCl (pH < 1.0).

2.2. Oxidation Experiments

Based on the conditions established by pre-experiments, working solutions of Fe(VI) and CBZ were prepared from dilution of the respective stock solutions. The working solutions of Fe(VI) were prepared using 10 mM phosphate or borate buffer with the pH adjusted by H_2SO_4 and NaOH prior to the addition of Fe(VI). The reaction was initiated by adding the Fe(VI) solution into the CBZ solution, and the changes in solution pH were less than ±0.1 during the reaction process. Unless noted otherwise, Fe(VI) oxidation of CBZ was conducted at pH 8.0 with the concentrations of Fe(VI) and CBZ at 150 μM and 10 μM, respectively. The solution pH (6.0 to 10.0), Fe(VI) concentration (0 to 200 μM), and CBZ concentration (10 to 50 μM) were varied when studying the influence of various factors on the degradation kinetics. The reaction mixtures were sampled (2 mL) and quenched with 20 μL of 1 M oxalic acid ($C_2H_2O_4$) to terminate the reaction at pre-determined time points. The solution samples were filtered using 0.22 μm PTFE membrane filters prior to analysis. In parallel, 10 mL solution samples were withdrawn for determination of the residual Fe(VI) concentrations using the ABTS method [42]. The degradation of CBZ by Fe(VI) oxidation was also investigated in natural water matrices. Tap water and lake water, which were obtained from a faucet and the Weiming Lake on the campus of Peking University (Beijing, China), respectively, were used to represent natural water of different quality (i.e., well-treated water and raw surface water). All Fe(VI) oxidation experiments were conducted at least in duplicate.

2.3. Analytical Methods

The concentration of CBZ was determined on an LC-20A High-Performance Liquid Chromatograph (HPLC, Shimadzu, Kyoto, Japan) with an SPD-M20A photo-diode array detector (DAD), and the detection wavelength was 230 nm. A WondaSil C18 column (4.6 × 250 mm, 5 μm) was used for analyte separation. The flow rate was 1.0 mL min^{-1}, and the column temperature was set at 40 °C. The mobile phase was water (containing 0.1% formic acid) and methanol at a ratio of 3:2. The organic degradation products of CBZ were identified using an LX50 Ultra-High-Pressure Liquid Chromatograph coupled to a Qsight 210 Triple Quad Mass Spectrometer (UHPLC-MS/MS, PerkinElmer, Waltham, MA, USA). The pH values of the sample solutions were adjusted to approximately 7.0 using $NH_3 \cdot H_2O$ and CH_3COOH to cause precipitation of ferric hydroxide, which was further removed from the solution with a 0.22 μm PTFE membrane filter. A TOC-V CPH analyzer (Shimadzu, Kyoto, Japan) was used to determine the total organic carbon (TOC) contents of the sample solutions.

2.4. Theoretical Calculations

The atomic partial charge distribution of CBZ molecule was obtained with theoretical calculations to explore the initial reaction site by Fe(VI) oxidation. Density functional theory (DFT) calculations were performed using the Gaussian 09 software package at the B3LYP/3-21G level.

3. Results and Discussion

3.1. CBZ Degradation in Fe(VI) Oxidation

The impact of Fe(VI) dose on CBZ degradation by Fe(VI) oxidation was first investigated with the molar ratio of Fe(VI) to CBZ ranging from 0:1 to 20:1. As shown in Figure 1a, the degradation of CBZ increased with the increase in Fe(VI) dose due to the presence of more oxidant. After 30 min of reaction, 95.9% ± 0.7% of CBZ was degraded at a Fe(VI)-to-CBZ molar ratio of 15:1, while a further increase in the Fe(VI)-to-CBZ molar ratio (20:1) barely improved CBZ degradation. Thus, a molar ratio of 15:1 is considered sufficient for the dose of Fe(VI) in the oxidation of CBZ. Solution pH is also an important factor in Fe(VI)

oxidation, as it influences the chemical speciation of both Fe(VI) and CBZ and, thus, the overall reactivity of Fe(VI) towards CBZ. To study the effect of solution pH, the degradation kinetics of CBZ by Fe(VI) oxidation was determined in the pH range of 6.0 to 10.0 at a Fe(VI)-to-CBZ molar ratio of 15:1. As shown in Figure 1b, the degradation of CBZ by Fe(VI) oxidation was 88.2% ± 1.3%, 70.7% ± 1.7%, 95.9% ± 0.7%, 79.2% ± 0.8%, and 41.0% ± 1.3% at pH 6.0, 7.0, 8.0, 9.0, and 10.0, respectively, in 30 min. The highest degradation of CBZ occurred at pH 8.0, which is attributable to the balance between the stability and oxidative power of Fe(VI) species in water under such conditions. Fe(VI) in aqueous solution is unstable and easily undergoes decomposition through a series of reactions, producing $Fe(OH)_3$, O_2, and H_2O_2 ($2HFe^{VI}O_4^- + 4H_2O \rightarrow 2H_3Fe^{IV}O_4^- + 2H_2O_2$; $HFe^{VI}O_4^- + H_2O_2 \rightarrow H_3Fe^{IV}O_4^- + O_2$; $H_3Fe^{IV}O_4^- + H_2O_2 + H^+ \rightarrow Fe^{II}(OH)_2 + O_2 + 2H_2O$; $HFe^{VI}O_4^- + Fe^{II}(OH)_2 + H_2O \rightarrow H_2Fe^{V}O_4^- + Fe^{III}(OH)_3$; $2H_2Fe^{V}O_4^- + 2H_2O + 2H^+ \rightarrow 2Fe^{III}(OH)_3 + 2H_2O_2$; $HFe^{V}O_4^{2-} + H_2O_2 + 2H^+ \rightarrow Fe^{III}(OH)_3 + O_2 + H_2O$) [43–46]. As the solution pH increases, Fe(VI) becomes more stable while its self-decomposition slows down [32]. On the other hand, the overall oxidative power of Fe(VI) decreases with the solution pH, as detailed later. In addition, the chemical speciation of both CBZ and Fe(VI) changes with the solution pH.

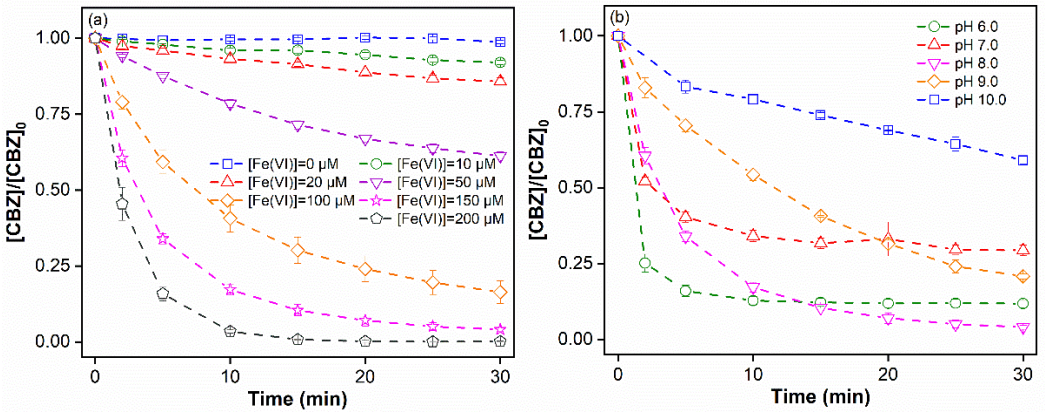

Figure 1. Influence of (**a**) Fe(VI) concentration and (**b**) solution pH on CBZ degradation in Fe(VI) oxidation. Experimental conditions: (**a**) pH = 8.0, $[CBZ]_0$ = 10 μM and $[Fe(VI)]_0$ = 0 to 200 μM; (**b**) pH = 6.0 to 10.0, $[CBZ]_0$ = 10 μM, and $[Fe(VI)]_0$ = 150 μM.

Since CBZ removal by Fe(VI) oxidation is affected by several factors, which may have interactions, the optimum reaction conditions of CBZ degradation by Fe(VI) oxidation were further determined through response surface optimization experiments. The pH was set in the range of 6.0 to 10.0, and the concentration of Fe(VI) was set between 100 and 200 μM. The results of the response surface optimization experiments (Figure 2) indicated that the optimum reaction conditions for the degradation of 10 μM CBZ in Fe(VI) oxidation are: pH = 7.8 and [Fe(VI)] = 150 μM. Under such conditions, 96.9% of the CBZ can be degraded in 30 min.

To further investigate the oxidation kinetics of CBZ oxidation by Fe(VI), the rate constants of the reaction between Fe(VI) and CBZ in the pH range of 6.2 to 10.0 were determined. Due to the potential involvement of Fe(IV)/Fe(V) during the degradation process of CBZ by Fe(VI) oxidation [47,48], the kinetic experiments were performed at much higher concentrations of CBZ than those of Fe(VI) to minimize their contribution. Under these conditions, the decay of Fe(VI) should obey pseudo-first-order kinetics, which can be expressed as:

$$-\frac{d[Fe(VI)]}{dt} = k_{app}[Fe(VI)][CBZ]_0^n = k_{obs}[Fe(VI)] \quad (1)$$

where k_{app} (M^{-1} s^{-1}) is the apparent rate constant of the reaction between Fe(VI) and CBZ, and k_{obs} (s^{-1}) is the pseudo-first-order rate constant of Fe(VI) decay. n represents the stoichiometric number of the reaction for CBZ, which can be calculated as:

$$\ln k_{obs} = \ln k_{app} + n \ln[CBZ]_0 \quad (2)$$

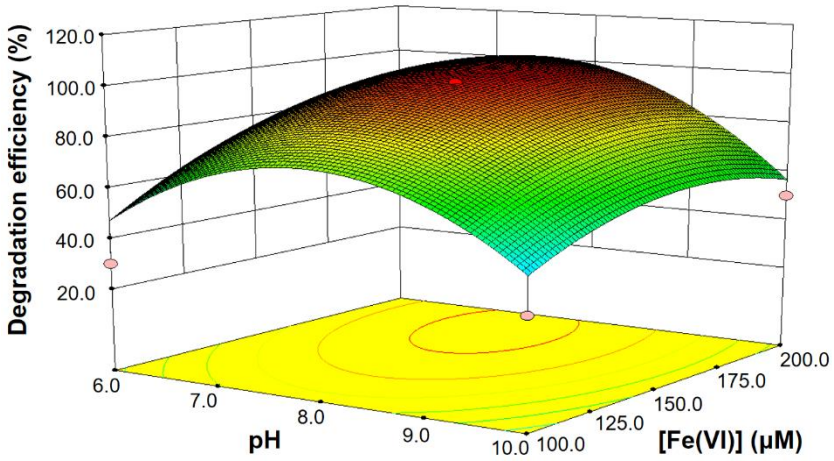

Figure 2. Response surface optimization results for CBZ degradation in Fe(VI) oxidation. Experimental conditions: pH = 6.0 to 10.0, $[CBZ]_0$ = 10 μM, and $[Fe(VI)]_0$ = 100 to 200 μM.

The decay of Fe(VI) can be well fitted with the pseudo-first-order kinetics at different solution pH values. The values of n (the slopes of $\ln k_{obs}$ vs. $\ln[CBZ]_0$) were close to 1.0 at each pH value, as shown in Figure 3a. These results indicate that the overall reaction between Fe(VI) and CBZ is second order. The k_{app} values of the reaction between Fe(VI) and CBZ were further determined according to Equation (2). k_{app} was found to be 88.0 ± 5.2, 77.7 ± 6.7, 62.9 ± 0.1, 36.0 ± 2.8, 10.7 ± 0.3, 5.5 ± 0.7, 2.3 ± 0.1, and 1.6 ± 0.3 M^{-1} s^{-1} at solution pH of 6.2, 6.5, 7.0, 7.5, 8.0, 8.5, 9.0, and 10.0, respectively. Figure 3b shows the pH dependence of k_{app}. The reduction in the overall reactivity of Fe(VI) towards CBZ can be attributed to the varying forms of Fe(VI) and CBZ in the solution under different pH conditions. Fe(VI) has three pK_a values ($H_3FeO_4^+ \rightleftharpoons H^+ + H_2FeO_4$, p$K_{a1}$ = 1.6 ± 0.2; $H_2FeO_4 \rightleftharpoons H^+ + HFeO_4^-$, p$K_{a2}$ = 3.5; $HFeO_4^- \rightleftharpoons H^+ + FeO_4^{2-}$, p$K_{a3}$ = 7.3 ± 0.1) [49], while the pK_a of CBZ has been reported to be 4.3 [19]. In the pH range of 6.0 to 12.0, Fe(VI) mainly exists in the form of $HFeO_4^-$ and FeO_4^{2-}, and the percentage of $HFeO_4^-$ decreases with the increase in solution pH, while CBZ mainly exists in the form of neutral molecules. The evolution of k_{app} for the reaction between Fe(VI) and CBZ with the solution pH can be modeled as:

$$k_{app} = \sum_{ij} k_{ij\alpha_i\beta_j} \quad (3)$$

where i and j are the number of chemical forms of Fe(VI) and CBZ existing in the solution system, respectively; k_{ij} is the species-specific, second-order rate constant of the reaction between the i-th Fe(VI) species and the j-th CBZ species; α_i is the fraction of i-th Fe(VI) species in total Fe(VI); and β_j is the fraction of j-th CBZ species in total CBZ. In the pH range of 6.0 to 12.0, Fe(VI) mainly exists in the form of $HFeO_4^-$ and FeO_4^{2-}, while CBZ mainly exists in the form of neutral molecules, and, thus, the values of i and j can be defined as 2 and 1, respectively. Based on the experimental data, the species-specific rate constant for the reaction between $HFeO_4^-$ and CBZ was calculated to be 95.5 M^{-1} s^{-1}, and that for the reaction between FeO_4^{2-} and CBZ was 0.6 M^{-1} s^{-1}. The much higher reaction rate constant of $HFeO_4^-$ towards CBZ (compared to that of FeO_4^{2-} towards CBZ) can be attributed to its much higher oxidative power [27,30,33]. With the increase in solution pH, the share of $HFeO_4^-$ decreased, causing a reduction in the overall rate of the reaction between Fe(VI) and CBZ (Figure 3b).

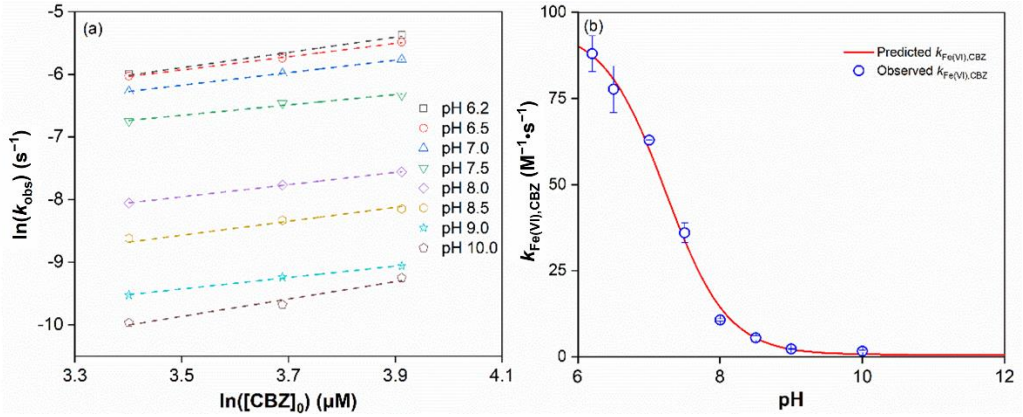

Figure 3. Reaction rate of CBZ with Fe(VI) under different solution pH conditions: (**a**) linear fitting between the natural logarithm of the observed reaction rate constant of CBZ degradation and that of CBZ concentration in Fe(VI) oxidation and (**b**) pH dependence of the observed rate constant of CBZ degradation in Fe(VI) oxidation. Experimental conditions: pH = 6.2 to 10.0, $[CBZ]_0$ = 30, 40, and 50 μM, and $[Fe(VI)]_0$ = 3.0 μM.

3.2. Effects of Inorganic Ions on CBZ Degradation in Fe(VI) Oxidation

Inorganic ions are widely present in surface water and wastewater, which may affect the degradation of CBZ in Fe(VI) oxidation. The effects of common cations (Na^+, K^+, NH_4^+, Ca^{2+}, Mg^{2+}, Cu^{2+}, and Fe^{3+}) and common anions (Cl^-, Br^-, NO_3^-, HCO_3^-, and SO_4^{2-}) on CBZ degradation in Fe(VI) oxidation were investigated. The concentrations of all inorganic ions were set as 1.0 mM, and the solution pH was set as 8.0. Figure 4a depicts the degradation kinetics of CBZ in Fe(VI) oxidation in the presence of various cations. The degradation of CBZ in Fe(VI) oxidation in 30 min was 95.9% ± 0.7% in ultrapure water and 97.7% ± 0.4%, 98.1% ± 0.3%, 96.7% ± 1.0%, 98.7% ± 0.6%, 97.4% ± 0.4%, 99.7% ± 0.1%, and 99.9% ± 0.0% in the presence of Na^+, K^+, NH_4^+, Ca^{2+}, Mg^{2+}, Cu^{2+}, and Fe^{3+}, respectively. Cu^{2+} and Fe^{3+} significantly accelerated the degradation of CBZ, while the presence of Na^+, K^+, NH_4^+, Ca^{2+}, and Mg^{2+} had no obvious impact. The effects of these common cations are similar to those observed in the transformation of 4-tert-butylphenol in Fe(VI) oxidation [39]. A recent study reported that Cu^{2+} significantly enhanced the removal of sulfamethoxazole in Fe(VI) oxidation and attributed the promoting role of Cu^{2+} to the production of highly reactive Fe(IV)/Fe(V) and Cu(III) species [50]. Other studies also reported that Cu^{2+} could enhance the degradation of organic pollutants in Fe(VI) oxidation [39,51,52]. Fe^{3+} can act as a reducing agent and reduce Fe(VI) to Fe(IV)/Fe(V); thus, its presence can accelerate CBZ degradation [52,53]. These results show that the presence of common inorganic cations does not compromise the performance of Fe(VI) oxidation in treating CBZ.

Figure 4b shows the impact of common inorganic anions on CBZ degradation in Fe(VI) oxidation. The degradation of CBZ in Fe(VI) oxidation in 30 min was 97.7% ± 0.4%, 97.8% ± 1.2%, 96.8% ± 0.4%, 98.1% ± 0.7%, and 94.9% ± 0.4% in the presence of Cl^-, Br^-, NO_3^-, HCO_3^-, and SO_4^{2-}, respectively. The negligible effect of inorganic anions on CBZ degradation in Fe(VI) oxidation was attributed to the low reactivity of Fe(VI) towards these inorganic anions [36,51,54,55]. It has been reported that HCO_3^- can form complexes with Fe(V) and suppress its decomposition, thus, enhancing the degradation of organic pollutants [56]. However, no significant effect of HCO_3^- was observed in this study, probably because Fe(V) played a minor role in the overall degradation of CBZ in Fe(VI) oxidation.

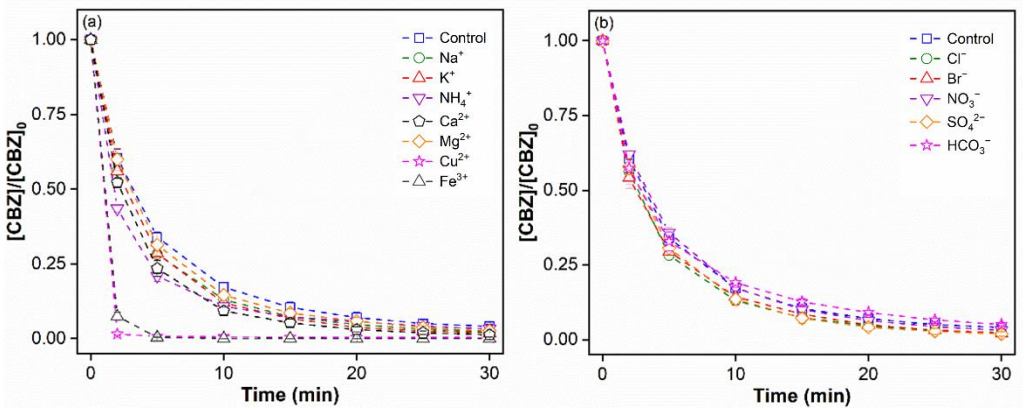

Figure 4. Influence of (**a**) common inorganic cations and (**b**) common inorganic anions on CBZ degradation in Fe(VI) oxidation. Experimental conditions: pH = 8.0, $[CBZ]_0$ = 10 μM, $[Fe(VI)]_0$ = 150 μM, and $[inorganic\ ion]_0$ = 1.0 mM.

3.3. Effects of HA and Water Matrices on CBZ Degradation in Fe(VI) Oxidation

HA is commonly used as a model for DOM, which is widely present in natural aquatic environment. It has been reported that the typical concentrations of HA are up to about 10.0 mg L^{-1} in surface water [57]. Due to its high redox activity, HA can be readily oxidized by many oxidants, such as active free radicals and Fe(VI). The effect of HA on CBZ degradation in Fe(VI) oxidation was investigated with the presence of 0, 1, 5, 10, and 20 mg L^{-1} HA. Figure 5a shows that HA in the concentration range of 0 to 20 mg L^{-1} accelerated the degradation of CBZ in Fe(VI) oxidation, which is consistent with the findings of previous studies on the influence of HA on pollutant degradation in Fe(VI) oxidation [33,39]. The accelerated CBZ degradation was attributed to the reduction of Fe(VI) by HA, which produces highly reactive Fe(IV)/Fe(V) species. The degradation of CBZ in Fe(VI) oxidation after 30 min was comparable in the solutions with different levels of HA added, which resulted from the fact that Fe(VI) was overdosed (Fe(VI)-to-CBZ molar ratio of 15:1) in the treatment systems.

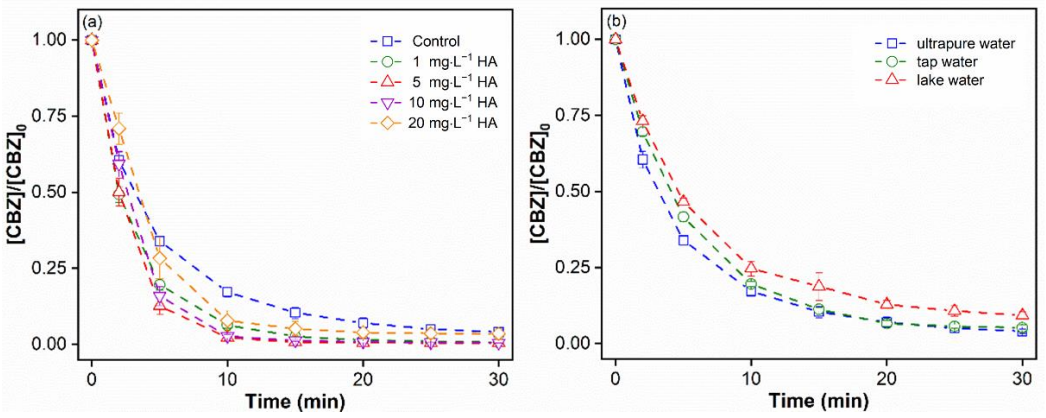

Figure 5. Influence of (**a**) HA and (**b**) water matrices on CBZ degradation in Fe(VI) oxidation. Experimental conditions: pH = 8.0, $[CBZ]_0$ = 10 μM, and $[Fe(VI)]_0$ = 150 μM.

Figure 5b compares the performance of Fe(VI) oxidation in degrading CBZ in different water matrices (ultrapure water, tap water, and lake water). The degradation of CBZ in tap water was close to that in ultrapure water, while CBZ degradation was apparently slower in lake water. This can be attributed to the fact that tap water has rather low contents of dissolved inorganic and organic species, while lake water has a much more complex matrix (with respect to both inorganic and organic species). Nonetheless, Fe(VI) oxidation performed reasonably well in degrading CBZ in lake water, demonstrating that Fe(VI)

oxidation is not significantly subjected to interference from co-existing ions and DOM in natural water matrices.

3.4. Pathways and Mechanism of CBZ Degradation in Fe(VI) Oxidation

Figure 6a shows the evolution of solution TOC during CBZ degradation in Fe(VI) oxidation. Relatively fast reduction in solution TOC occurred within the first 5 min, while the change was insignificant after that. The fast TOC removal at the beginning of the reaction was attributed to the high initial concentration of Fe(VI). The TOC removal was only 27.5% ± 1.0% after 30 min of treatment, indicating that full mineralization of CBZ cannot occur in Fe(VI) oxidation. It has been reported that the benzimidazole ring is stable and not prone to being attacked by oxidants, such as •OH [58]. Seven organic degradation products of CBZ attacked by Fe(VI) were identified using UHPLC-MS/MS. Figure 6b shows the proposed degradation pathways of CBZ in Fe(VI) oxidation based on the organic degradation products identified. The main degradation pathways include hydroxylation, removal of the methoxyl group, and the cleavage of C–N/C=N bond. First, the CBZ molecule transfers one electron to Fe(VI) and forms the corresponding organic radical, which further goes through hydroxylation to form P1 (m/z = 207.96) or removal of the methoxyl group to form P2 (m/z = 159.96). Subsequently, P1 can undergo hydroxylation to produce P3 (m/z = 223.88), while hydroxylation of P2 yields P4 (m/z = 175.98). Cleavage of the C=N bond on P2 results in P5 (m/z = 133.88), the $–NH_2$ group of which can be further cleaved off to yield P6 (m/z = 118.87). The imidazole ring of P4 and P6 may go through cleavage to produce P7 (m/z = 108.90). Further degradation of P7 under the attack of Fe(VI) yields small degradation products and, eventually, CO_2 and H_2O. It is worth noting that the full mineralization of CBZ was not achieved by Fe(VI) oxidation, which is similar to the results observed in the treatment of CBZ by other types of AOPs reported in the literature [19,23,59]. Due to the lack of standard substances, we were not able to quantify the concentrations of degradation intermediates of CBZ or test their toxicity. Further study should be conducted to evaluate the stability of these major degradation intermediates and assess their human health risk. All the Fe(VI) added into the treatment system would eventually transform into $Fe(OH)_3$ through oxidizing the organic species or self-decomposition; thus, no residue of Fe(VI) is expected in the treated solution.

To further investigate the degradation mechanism of CBZ in Fe(VI) oxidation, DFT calculations were employed to explore the initial reaction site on CBZ molecule under the attack of Fe(VI) [58,60]. Fe(VI) is an electrophilic oxidant, which reacts with organic pollutants mainly through electron transfer. Figure 7 depicts the calculated atomic partial charge distribution of the CBZ molecule. The N atom on the amide group has the highest charge density; thus, this site is expected to be preferentially attacked by Fe(VI). This result further corroborates the initial degradation step of CBZ under the attack of Fe(VI) in the proposed degradation pathways (Figure 6b).

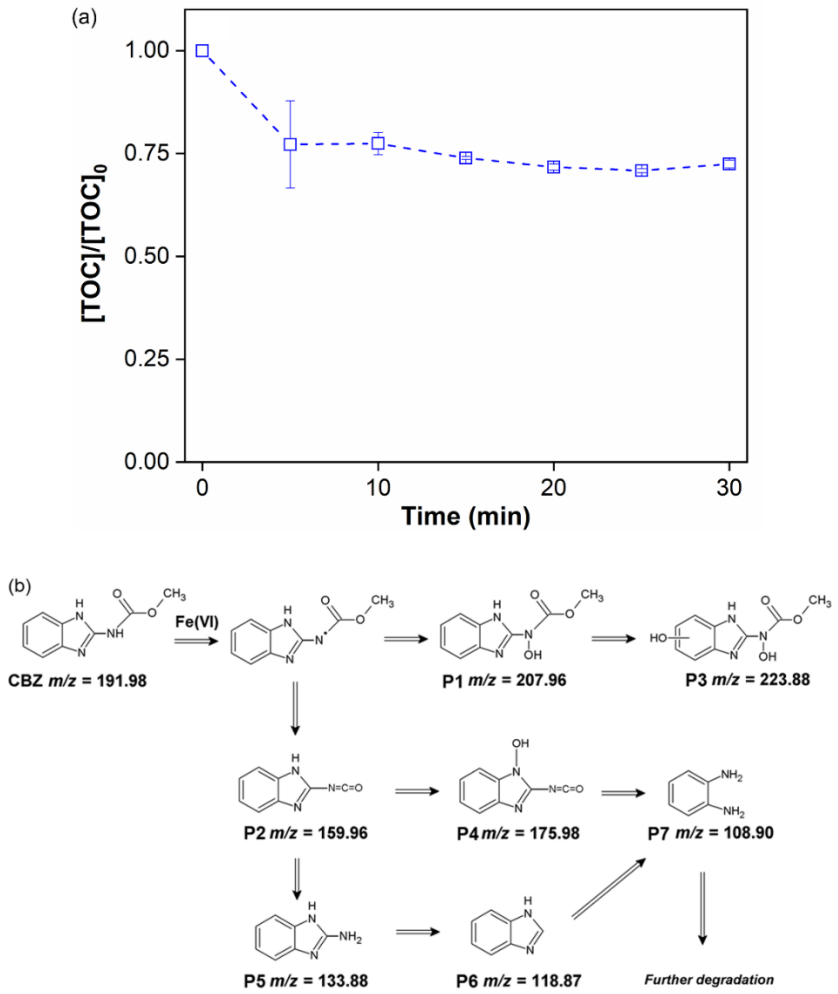

Figure 6. Mineralization of CBZ and the degradation pathways in Fe(VI) oxidation: (**a**) solution TOC evolution and (**b**) proposed degradation pathways of CBZ. Experimental conditions: pH = 8.0, $[CBZ]_0$ = 10 μM, and $[Fe(VI)]_0$ = 150 μM.

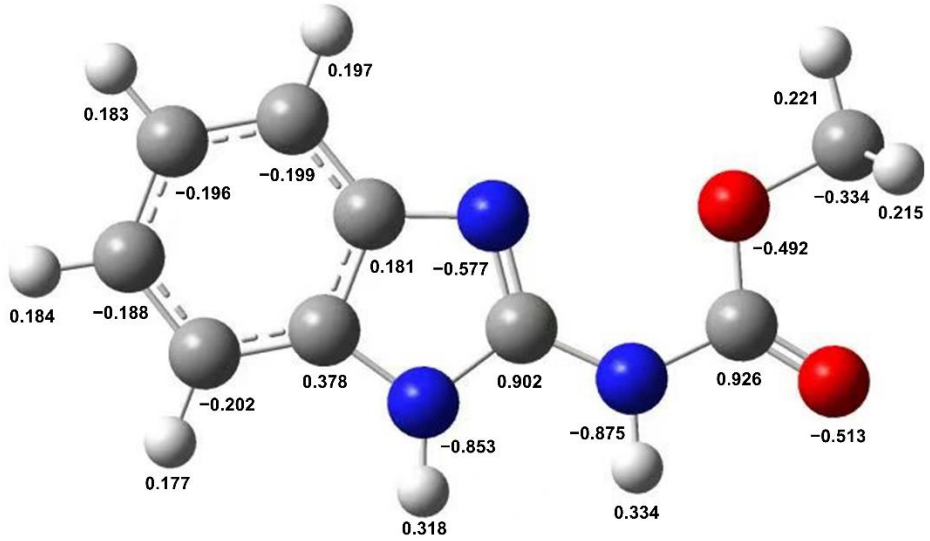

Figure 7. Atomic partial charge distribution of CBZ molecule obtained by DFT calculations.

4. Conclusions

The results of this study show that Fe(VI) oxidation could efficiently remove CBZ from water under near-neutral conditions. Under the optimum conditions of pH = 7.8 and [Fe(VI)]/[CBZ] = 14.2 (in molarity), 96.9% of CBZ were removed after 30 min of Fe(VI) oxidation. The reaction between Fe(VI) and CBZ could be well described with second-order kinetics, and the overall rate constant decreases with the increase in solution pH. The removal of CBZ could be accelerated by Cu^{2+} and Fe^{3+}, while common cations (Na^+, K^+, Ca^{2+}, Mg^{2+}, and NH_4^+) and common anions (Cl^-, Br^-, NO_3^-, SO_4^{2-}, and HCO_3^-) showed negligible influence. The presence of HA at low concentrations accelerated CBZ degradation in Fe(VI) oxidation due to the formation of highly reactive Fe(IV)/Fe(V) species from the reduction of Fe(VI) by HA. CBZ in tap water and lake water was also be efficiently removed by Fe(VI) oxidation, demonstrating that the treatment performance is not strongly influenced by water matrices. The degradation pathways of CBZ by Fe(VI) oxidation mainly include hydroxylation, removal of the methoxyl group, and cleavage of the C–N/C=N bond, and the initial reaction site is the N atom of the amide group on CBZ molecule. These findings could help guide the development of a practical treatment technology based on Fe(VI) oxidation for CBZ and other benzimidazole fungicides in natural water and wastewater.

Author Contributions: Y.L.: conceptualization, data curation, methodology, writing—original draft, writing—review and editing; H.C.: conceptualization, funding acquisition, resources, supervision, writing—original draft, writing—review and editing. All authors have read and agreed to the published version of the manuscript.

Funding: This research was funded by the Natural Science Foundation of China (grant nos. U2006212 and 41725015).

Institutional Review Board Statement: Not applicable.

Informed Consent Statement: Not applicable.

Data Availability Statement: The data presented in this study are available upon reasonable request.

Conflicts of Interest: The authors declare no conflict of interest.

References

1. Merel, S.; Benzing, S.; Gleiser, C.; Di Napoli-Davis, G.; Zwiener, C. Occurrence and overlooked sources of the biocide carbendazim in wastewater and surface water. *Environ. Pollut.* **2018**, *239*, 512–521. [CrossRef] [PubMed]
2. Zhu, Z.; Zhou, F.; Li, J.; Zhu, F.; Ma, H. Carbendazim resistance in field isolates of Sclerotinia sclerotiorum in China and its management. *Crop Prot.* **2016**, *81*, 115–121. [CrossRef]
3. Rizzi, V.; Gubitosa, J.; Fini, P.; Romita, R.; Agostiano, A.; Nuzzo, S.; Cosma, P. Commercial bentonite clay as low-cost and recyclable "natural" adsorbent for the carbendazim removal/recover from water: Overview on the adsorption process and preliminary photodegradation considerations. *Colloids Surfaces A Physicochem. Eng. Asp.* **2020**, *602*, 125060. [CrossRef]
4. Singh, S.; Singh, N.; Kumar, V.; Datta, S.; Wani, A.B.; Singh, D.; Singh, K.; Singh, J. Toxicity, monitoring and biodegradation of the fungicide carbendazim. *Environ. Chem. Lett.* **2016**, *14*, 317–329. [CrossRef]
5. Boudina, A.; Emmelin, C.; Baaliouamer, A.; Grenier-Loustalot, M.F.; Chovelon, J.M. Photochemical behaviour of carbendazim in aqueous solution. *Chemosphere* **2003**, *50*, 649–655. [CrossRef]
6. Pourreza, N.; Rastegarzadeh, S.; Larki, A. Determination of fungicide carbendazim in water and soil samples using dispersive liquid-liquid microextraction and microvolume UV–vis spectrophotometry. *Talanta* **2015**, *134*, 24–29. [CrossRef]
7. Chen, Z.; Ying, G.; Liu, Y.; Zhang, Q.; Zhao, J.; Liu, S.; Chen, J.; Peng, F.; Lai, H.; Pan, C. Triclosan as a surrogate for household biocides: An investigation into biocides in aquatic environments of a highly urbanized region. *Water Res.* **2014**, *58*, 269–279. [CrossRef]
8. Liu, W.; Zhao, J.; Liu, Y.; Chen, Z.; Yang, Y.; Zhang, Q.; Ying, G. Biocides in the Yangtze River of China: Spatiotemporal distribution, mass load and risk assessment. *Environ. Pollut.* **2015**, *200*, 53–63. [CrossRef]
9. Wang, A.; Mahai, G.; Wan, Y.; Jiang, Y.; Meng, Q.; Xia, W.; He, Z.; Xu, S. Neonicotinoids and carbendazim in indoor dust from three cities in China: Spatial and temporal variations. *Sci. Total Environ.* **2019**, *695*, 133790. [CrossRef]
10. Campos-Mañas, M.C.; Plaza-Bolaños, P.; Martínez-Piernas, A.B.; Sánchez-Pérez, J.A.; Agüera, A. Determination of pesticide levels in wastewater from an agro-food industry: Target, suspect and transformation product analysis. *Chemosphere* **2019**, *232*, 152–163. [CrossRef]

11. Ramírez-Morales, D.; Pérez-Villanueva, M.E.; Chin-Pampillo, J.S.; Aguilar-Mora, P.; Arias-Mora, V.; Masís-Mora, M. Pesticide occurrence and water quality assessment from an agriculturally influenced Latin-American tropical region. *Chemosphere* **2021**, *262*, 127851. [CrossRef] [PubMed]
12. Xu, L.; Granger, C.; Dong, H.; Mao, Y.; Duan, S.; Li, J.; Qiang, Z. Occurrences of 29 pesticides in the Huangpu River, China: Highest ecological risk identified in Shanghai metropolitan area. *Chemosphere* **2020**, *251*, 126411. [CrossRef] [PubMed]
13. Wan, Y.; Tran, T.M.; Nguyen, V.T.; Wang, A.; Wang, J.; Kannan, K. Neonicotinoids, fipronil, chlorpyrifos, carbendazim, chlorotriazines, chlorophenoxy herbicides, bentazon, and selected pesticide transformation products in surface water and drinking water from northern Vietnam. *Sci. Total Environ.* **2021**, *750*, 141507. [CrossRef]
14. Liu, S.; Yang, R.; Chen, H.; Fu, Q. Residue and degradation of carbendazim in rice and soil. *J. Agro Environ. Sci.* **2011**, *31*, 357–361.
15. Daam, M.A.; Garcia, M.V.; Scheffczyk, A.; Rombke, J. Acute and chronic toxicity of the fungicide carbendazim to the earthworm Eisenia fetida under tropical versus temperate laboratory conditions. *Chemosphere* **2020**, *255*, 126871. [CrossRef]
16. Fan, R.; Zhang, W.; Li, L.; Jia, L.; Zhao, J.; Zhao, Z.; Peng, S.; Yuan, X.; Chen, Y. Individual and synergistic toxic effects of carbendazim and chlorpyrifos on zebrafish embryonic development. *Chemosphere* **2021**, *280*, 130769. [CrossRef]
17. Baigorria, E.; Fraceto, L.F. Novel nanostructured materials based on polymer/organic-clay composite networks for the removal of carbendazim from waters. *J. Clean. Prod.* **2022**, *331*, 129867. [CrossRef]
18. Li, Y.; Cheng, H. Chemical kinetic modeling of organic pollutant degradation in Fenton and solar photo-Fenton processes. *J. Taiwan Inst. Chem. Eng.* **2021**, *123*, 175–184.
19. Machado, R.M.; da Silva, S.W.; Bernardes, A.M.; Ferreira, J.Z. Degradation of carbendazim in aqueous solution by different settings of photochemical and electrochemical oxidation processes. *J. Environ. Manag.* **2022**, *310*, 114805. [CrossRef]
20. Xie, X.; Hu, Y.; Cheng, H. Rapid degradation of *p*-arsanilic acid with simultaneous arsenic removal from aqueous solution using Fenton process. *Water Res.* **2016**, *89*, 59–67.
21. da Costa, E.P.; Bottrel, S.E.C.; Starling, M.C.V.M.; Leão, M.M.D.; Amorim, C.C. Degradation of carbendazim in water via photo-Fenton in raceway pond reactor: Assessment of acute toxicity and transformation products. *Environ. Sci. Pollut. Res.* **2019**, *26*, 4324–4336. [CrossRef] [PubMed]
22. Mazellier, P.; Leroy, E.; De Laat, J.; Legube, B. Degradation of carbendazim by UV/H_2O_2 investigated by kinetic modelling. *Environ. Chem. Lett.* **2003**, *1*, 68–72. [CrossRef]
23. Kaur, T.; Sraw, A.; Wanchoo, R.K.; Toor, A.P. Solar assisted degradation of carbendazim in water using clay beads immobilized with TiO_2 & Fe doped TiO_2. *Sol. Energy* **2018**, *162*, 45–56.
24. Xu, L.; Dong, H.; Xu, K.; Li, J.; Qiang, Z. Accelerated degradation of pesticide by permanganate oxidation: A comparison of organic and inorganic activations. *Chem. Eng. J.* **2019**, *369*, 1119–1128. [CrossRef]
25. Sharma, V.K.; Zboril, R.; Varma, R.S. Ferrates: Greener oxidants with multimodal action in water treatment technologies. *Acc. Chem. Res.* **2015**, *48*, 182–191. [CrossRef]
26. Sharma, V.K.; Chen, L.; Zboril, R. Review on high valent Fe^{VI} (ferrate): A sustainable green oxidant in organic chemistry and transformation of pharmaceuticals. *ACS Sustain. Chem. Eng.* **2016**, *4*, 18–34. [CrossRef]
27. Dai, M.; Luo, Z.; Luo, Y.; Zheng, Q.; Zhang, B. Degradation of 2,6-dichlorophenol by ferrate(VI) oxidation: Kinetics, performance, and mechanism. *Sep. Purif. Technol.* **2021**, *278*, 119475. [CrossRef]
28. Dong, F.; Li, J.; Lin, Q.; Wang, D.; Li, C.; Shen, Y.; Zeng, T.; Song, S. Oxidation of chloroquine drug by ferrate: Kinetics, reaction mechanism and antibacterial activity. *Chem. Eng. J.* **2020**, *428*, 131408. [CrossRef]
29. Liu, H.; Pan, X.; Chen, J.; Qi, Y.; Qu, R.; Wang, Z. Kinetics and mechanism of the oxidative degradation of parathion by ferrate(VI). *Chem. Eng. J.* **2019**, *365*, 142–152. [CrossRef]
30. Sharma, V.K. Ferrate(VI) and ferrate(V) oxidation of organic compounds: Kinetics and mechanism. *Coord. Chem. Rev.* **2013**, *257*, 495–510. [CrossRef]
31. Wang, K.; Shu, J.; Sharma, V.K.; Liu, C.; Xu, P.; Nesnas, N.; Wang, H. Unveiling the mechanism of imidacloprid removal by ferrate(VI): Kinetics, role of oxidation and adsorption, reaction pathway and toxicity assessment. *Sci. Total Environ.* **2022**, *805*, 150383. [CrossRef] [PubMed]
32. Xie, X.; Cheng, H. A simple treatment method for phenylarsenic compounds: Oxidation by ferrate(VI) and simultaneous removal of the arsenate released with in situ formed Fe(III) oxide-hydroxide. *Environ. Int.* **2019**, *127*, 730–741. [CrossRef] [PubMed]
33. Chen, J.; Xu, X.; Zeng, X.; Feng, M.; Qu, R.; Wang, Z.; Nesnas, N.; Sharma, V.K. Ferrate(VI) oxidation of polychlorinated diphenyl sulfides: Kinetics, degradation, and oxidized products. *Water Res.* **2018**, *143*, 1–9. [CrossRef] [PubMed]
34. Feng, M.; Baum, J.C.; Nesnas, N.; Lee, Y.; Huang, C.H.; Sharma, V.K. Oxidation of sulfonamide antibiotics of six-membered heterocyclic moiety by ferrate(VI): Kinetics and mechanistic insight into SO_2 extrusion. *Environ. Sci. Technol.* **2019**, *53*, 2695–2704. [CrossRef] [PubMed]
35. Sun, S.; Liu, Y.; Ma, J.; Pang, S.; Huang, Z.; Gu, J.; Gao, Y.; Xue, M.; Yuan, Y.; Jiang, J. Transformation of substituted anilines by ferrate(VI): Kinetics, pathways, and effect of dissolved organic matter. *Chem. Eng. J.* **2018**, *332*, 245–252. [CrossRef]
36. Feng, M.; Wang, X.; Chen, J.; Qu, R.; Sui, Y.; Cizmas, L.; Wang, Z.; Sharma, V.K. Degradation of fluoroquinolone antibiotics by ferrate(VI): Effects of water constituents and oxidized products. *Water Res.* **2016**, *103*, 48–57. [CrossRef]
37. Yang, B.; Ying, G.; Zhao, J.; Liu, S.; Zhou, L.; Chen, F. Removal of selected endocrine disrupting chemicals (EDCs) and pharmaceuticals and personal care products (PPCPs) during ferrate(VI) treatment of secondary wastewater effluents. *Water Res.* **2012**, *46*, 2194–2204. [CrossRef]

38. Jiang, J.; Durai, H.B.P.; Winzenbacher, R.; Petri, M.; Seitz, W. Drinking water treatment by in situ generated ferrate(VI). *Desalination Water Treat.* **2015**, *55*, 731–739. [CrossRef]
39. Zheng, Q.; Wu, N.; Qu, R.; Albasher, G.; Cao, W.; Li, B.; Alsultan, N.; Wang, Z. Kinetics and reaction pathways for the transformation of 4-tert-butylphenol by ferrate(VI). *J. Hazard. Mater.* **2021**, *401*, 123405. [CrossRef]
40. Li, C.; Li, X.Z.; Graham, N. A study of the preparation and reactivity of potassium ferrate. *Chemosphere* **2005**, *61*, 537–543. [CrossRef]
41. Bielski, B.H.J.; Thomas, M.J. Studies of hypervalent iron in aqueous solutions. 1. Radiation-induced reduction of iron(VI) to iron(V) by CO_2^-. *J. Am. Chem. Soc.* **1987**, *109*, 7761–7764. [CrossRef]
42. Lee, Y.; Yoon, J.; von Gunten, U. Spectrophotometric determination of ferrate (Fe(VI)) in water by ABTS. *Water Res.* **2005**, *39*, 1946–1953. [CrossRef] [PubMed]
43. Rush, J.D.; Bielski, B.H.J. Kinetics of ferrate(V) decay in aqeuous solution. *Inorg. Chem.* **1989**, *28*, 3947–3951. [CrossRef]
44. Rush, J.D.; Bielski, B.H.J. Decay of ferrate(V) in neutral and acidic solutions. A premix pulse radiolysis study. *Inorg. Chem.* **1994**, *33*, 5499–5502. [CrossRef]
45. Rush, J.D.; Zhao, Z.; Bielski, B.H.J. Reaction of ferrate(VI)/ferrate(V) with hydrogen peroxide and superoxide anion- a stopped-flow and premix pulse radiolysis study. *Free. Radic. Res.* **1996**, *24*, 187–198. [CrossRef]
46. Lee, Y.; Kissner, R.; von Gunten, U. Reaction of ferrate(VI) with ABTS and self-decay of ferrate(VI): Kinetics and mechanisms. *Environ. Sci. Technol.* **2014**, *48*, 5154–5162. [CrossRef]
47. Wang, S.; Deng, Y.; Shao, B.; Zhu, J.; Hu, Z.; Guan, X. Three kinetic patterns for the oxidation of emerging organic contaminants by Fe(VI): The critical roles of Fe(V) and Fe(IV). *Environ. Sci. Technol.* **2021**, *55*, 11338–11347. [CrossRef]
48. Zhu, J.; Yu, F.; Meng, J.; Shao, B.; Dong, H.; Chu, W.; Cao, T.; Wei, G.; Wang, H.; Guan, X. Overlooked role of Fe(IV) and Fe(V) in organic contaminant oxidation by Fe(VI). *Environ. Sci. Technol.* **2020**, *54*, 9702–9710. [CrossRef]
49. Sharma, V.K. Potassium ferrate(VI): An environmentally friendly oxidant. *Adv. Environ. Res.* **2002**, *6*, 143–156. [CrossRef]
50. Shi, Z.; Wang, D.; Gao, Z.; Ji, X.; Zhang, J.; Jin, C. Enhanced ferrate oxidation of organic pollutants in the presence of Cu(II) Ion. *J. Hazard. Mater.* **2022**, *433*, 128772. [CrossRef]
51. Yang, B.; Ying, G. Oxidation of benzophenone-3 during water treatment with ferrate(VI). *Water Res.* **2013**, *47*, 2458–2466. [CrossRef] [PubMed]
52. Zhao, J.; Wang, Q.; Fu, Y.; Peng, B.; Zhou, G. Kinetics and mechanism of diclofenac removal using ferrate(VI): Roles of Fe^{3+}, Fe^{2+}, and Mn^{2+}. *Environ. Sci. Pollut. Res.* **2018**, *25*, 22998–23008. [CrossRef] [PubMed]
53. Zhang, X.; Feng, M.; Luo, C.; Nesnas, N.; Huang, C.H.; Sharma, V.K. Effect of metal ions on oxidation of micropollutants by ferrate(VI): Enhancing role of Fe^{IV} species. *Chem. Eng. J.* **2021**, *55*, 623–633. [CrossRef] [PubMed]
54. Manoli, K.; Nakhla, G.; Ray, A.K.; Sharma, V.K. Oxidation of caffeine by acid-activated ferrate(VI): Effect of ions and natural organic matter. *AIChE J.* **2017**, *63*, 4998–5006. [CrossRef]
55. Schreyer, J.M.; Ockerman, L.T. Stability of the ferrate(VI) ion in aqueous solution. *Anal. Chem.* **1951**, *23*, 1312–1314. [CrossRef]
56. Luo, C.; Feng, M.; Sharma, V.K.; Huang, C.-H. Oxidation of pharmaceutials by ferrate(VI) in hydrolyzed urine: Effects of major inorganic constituents. *Environ. Sci. Technol.* **2019**, *53*, 5272–5281. [CrossRef] [PubMed]
57. Ge, F.; Shu, H.; Dai, Y. Removal of bromide by aluminium chloride coagulant in the presence of humic acid. *J. Hazard. Mater.* **2007**, *147*, 457–462. [CrossRef]
58. Liu, W.; Li, Y.; Wang, Y.; Zhao, Y.; Xu, Y.; Liu, X. DFT insights into the degradation mechanism of carbendazim by hydroxyl radicals in aqueous solution. *J. Hazard. Mater.* **2022**, *431*, 128577. [CrossRef]
59. Kaur, T.; Toor, A.P.; Wanchoo, R.K. Parametric study on degradation of fungicide carbendazim in dilute aqueous solutions using nano TiO_2. *Desalination Water Treat.* **2014**, *54*, 122–131. [CrossRef]
60. Xiao, R.; Gao, L.; Wei, Z.; Spinney, R.; Luo, S.; Tang, C.; Yang, W. Mechanistic insight into degradation of endocrine disrupting chemical by hydroxyl radical: An experimental and theoretical approach. *Environ. Pollut.* **2017**, *231*, 1446–1452. [CrossRef]